

S. E. Burke  
S. L. Andrecyk  
R. Palepu

## Thermodynamic and aggregation properties of sodium dodecyl sulfate in aqueous binary mixtures of isomeric butanediols

Received: 5 July 2000  
Accepted: 25 July 2000

S. E. Burke · S. L. Andrecyk  
R. Palepu (✉)  
Department of Chemistry  
St. Francis Xavier University, Antigonish  
Nova Scotia B2G 2W5, Canada  
e-mail: rpalepu@stfx.ca  
Fax: + 1-902-8672414

**Abstract** The effect of aqueous binary mixtures of isomeric butanediols on the micellization of sodium dodecyl sulfate has been investigated. Conductivity and fluorescence techniques were employed to determine the critical micellar concentration, the degree of dissociation of the counterions and the aggregation numbers of the surfactants in these binary blends. Differential conductivity plots were employed to distinguish between the cooperative and the stepwise aggregation process of the surfactant in each solvent system. The mass-action model was employed to calculate the

hydrophobic and the electrostatic contributions to the Gibbs energy of micellization as well as the monomer and the counterion concentrations in the postmicellar region. The thermodynamic parameters calculated for each system indicate that the micellization process occurs more readily in the presence of cosolvent owing to the formation of mixed micelles.

**Key words** Sodium dodecyl sulfate · Butanediols · Fluorescence techniques · Thermodynamics and micellar properties

### Introduction

Commercial cleaners for lubrication and grease-stripping applications normally contain halogenated solvents in their formulations. Halogenated substances are generally toxic and pose a threat to the biosphere. It has become imperative in recent years to develop formulations that are nontoxic, biodegradable, inexpensive and environmentally friendly. The blending of water with various polar organic solvents along with common surfactants may prove to be an effective formulation for various cleaning operations [1].

Applications of surfactants in areas such as lubrication require water-free or water-poor media and hence the surfactant aggregation process in nonaqueous media has attracted considerable interest in recent years. Polar solvents with properties resembling those of water, such as ethylene glycol, glycerol and formamide, have been employed [2, 3]. It has been established from previous studies that the solvent system must have three charac-

teristics for amphiphilic aggregation to occur: (a) the solvent system must possess (b) high cohesive energy, (c) high dielectric constant and hydrogen bonding ability [4]. Numerous studies have been carried out on the aggregation process of surfactants when water is gradually replaced with other polar solvents. A number of solvents, such as glycerol [5–7], formamide [7–9] and ethylene glycol [10–16], have been investigated. Micellar properties in blended aqueous alcohol systems were also studied extensively, in view of the importance of alcohols as cosurfactants in microemulsions [17] and their use in the mobile phases in micellar liquid chromatography [18] as well as in micellar electrokinetic chromatography [19]. In the latter techniques critical micellar concentration (cmc) values are necessary to predict solute retention and, hence, the separation selectivity [20].

The recent interest in alcohol/micelle systems stems from the ability to examine the effect of hydrophobic interaction on micelle formation. This is accomplished

by investigating the micellar properties of ionic surfactants in aqueous solutions containing alcohol. The solvent hydrophobicity changes depending upon the particular alcohol employed, resulting in a change in the cmc values.

A significant amount of work dealing with the properties of *n*-alcohols with ionic surfactants has been reported in the literature [2, 3]; however, research on the interactions of alkanediols with micelles has been scarce [21–25].

As part of a comprehensive study on the micellar process in mixed solvent systems [6, 15, 16, 24, 25], we report here the micellar and thermodynamic properties of sodium dodecyl sulfate (SDS) in binary aqueous mixtures of isomeric 1,2-, 1,3-, 1,4- and 2,3-butanediols (BTDS). The study of isomeric BTDS was undertaken to examine the influence of the position of the second hydroxyl group on the backbone of the alkane chain on the micellar properties.

In the present study we determined the values of micellar properties such as the cmc, the effective degree of dissociation ( $\alpha$ ), the aggregation numbers ( $N_s$ ), the surface area of the headgroup ( $a_0$ ), the micellar radius ( $R_0$ ) and the critical packing parameters as a function of diol content in the binary mixture. Conductometric, potentiometric and fluorescence methods were employed for the determination of these properties. Complete thermodynamic properties of micellization and intermicellar properties were obtained by employing the mass-action model.

## Experimental

### Materials

SDS was obtained from BDH, recrystallized from methanol, further purified by Soxhlet extraction with diethyl ether for 72–100 h, and dried under vacuum. The BTDS were obtained from Aldrich with a stated purity of 99% plus and were used without further purification. Pyrene (Aldrich) was purified by sublimation followed by crystallization from ethanol. Hexadecylpyridinium chloride, used as a quencher in the fluorescence measurements, was purified by repeated crystallization from acetone. The water used to make solutions was obtained from a Millipore-Super Q system with a specific conductance less than  $2 \mu\text{Scm}^{-1}$ .

### Measurements

Specific conductance measurements of 15–20 different concentrations of SDS at fixed aqueous BTD compositions were made in a thermostated jacketed beaker, with a dip cell having a cell constant of  $1.02 \text{ cm}^{-1}$ . An automatic conductivity CDM 83 bridge (Radiometer) operating at 1000 Hz was employed. The accuracy of the conductance measurements was  $\pm 0.2\%$ .

A Fisher sodium ion selective electrode coupled with a double-junction reference electrode (Fisher 13-620-47) was used to measure the sodium ion activities. To prevent the precipitation of potassium dodecyl sulfate at the junction of the reference electrode, potassium nitrate solution was replaced by ammonium nitrate solution in the outer chamber.

The micropolarity of the probe's residential area in the micelles and that of the solvent mixture was determined from the  $I_1/I_3$  intensity ratio of the pyrene vibronic spectra. Pyrene fluorescence measurements were carried out using a Perkin-Elmer MPF66 fluorescence spectrophotometer. The pyrene concentration was fixed at  $1.0 \times 10^{-6} \text{ M}$  and the fluorophore was excited at a wavelength of 340 nm. The excitation slit width was 1.5 nm, while the emission slit was maintained at a width of 2.0 nm. The emission spectrum was scanned over the range 360–500 nm. In the determination of aggregation numbers, the concentration of the quencher, hexadecylpyridinium chloride, was held low enough so not to interfere with the assembly of the micelle.

The monomer, counterion and micelle concentration in the postmicellar region were calculated using a computer program based on the mass-action model as outlined by Moroi [26]. From these parameters, the free-energy contributions from the hydrophobic and electrostatic effects to the Gibbs micellization energy were calculated. The input parameters required for these calculations are aggregation numbers, cmc values and the degree of counterion binding by the micelles. These parameters were obtained using static fluorescence quenching, conductometric and potentiometric methods.

## Results and discussion

### cmc and degree of dissociation

The cmc values for SDS in the binary aqueous mixtures of BTDS were obtained by plotting specific conductance versus surfactant concentration. The breakpoint on the plot is taken as the cmc. A number of these plots for various percentages of 1,2-BTD in the binary mixtures are shown in Fig. 1. From these plots, the effective degree of counterion dissociation ( $\alpha$ ) is obtained from the ratios of the slope of the postmicellar region to that in the premicellar region. In all cases, smaller curvatures appeared around the cmc at higher diol concentrations and consequently the cmc and  $\alpha$  values were obtained with a slightly greater uncertainty.

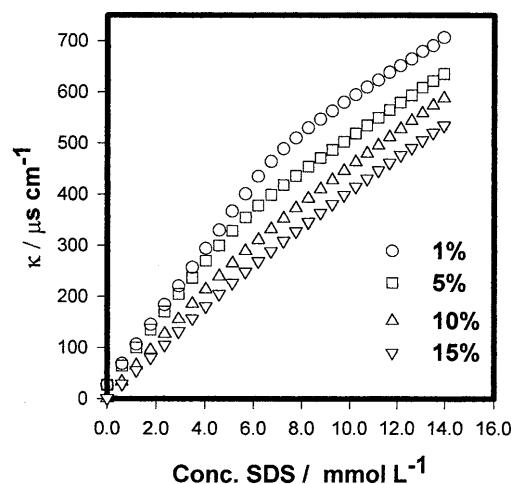


Fig. 1 Specific conductance versus concentration of sodium dodecyl sulfate (SDS) in aqueous mixtures of 1,2-butanediol (1,2-BTD)

When differential equivalence conductivity ( $\Delta\Lambda$ ),

$$\Delta\Lambda = 10^{-3} \frac{K_1 - K_1^i}{c_1 - c_1^i}, \quad (1)$$

is plotted versus mean concentration,  $c' = (c_1 - c_1^i)/2$ , a vertical decrease over a narrow concentration range is observed at lower diol concentration (Fig. 2A). This is attributed to a cooperative micellization process. However at higher diol content, the decrease is over a wider range of concentrations and this is indicative of a more gradual association prior to the micellization process (Fig. 2B).

The plots of the electromotive force versus the logarithm of the SDS concentration obtained from potentiometric measurements are shown in Fig. 3. The breakpoints in these plots correspond to cmc values and the values of  $\alpha$  were calculated as described in a previous publication [27].

More accurate cmc values at higher diol content were obtained by employing the pyrene  $I_1/I_3$  ratio method [28–30]. This procedure is based upon the sensitivity of the pyrene vibrational structure to the microenvironment of the probe. Below the cmc, with no micelles in the system, the  $I_1/I_3$  ratio corresponds to a polar environment. In the presence of micelles it is well known that the probe resides in the palisade layer of the micelle,

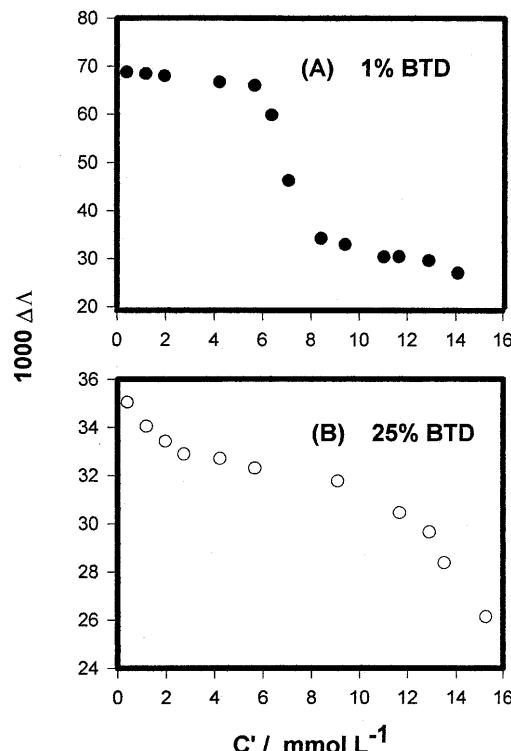


Fig. 2 Differential equivalent conductance versus mean concentration of 1,4-BTD

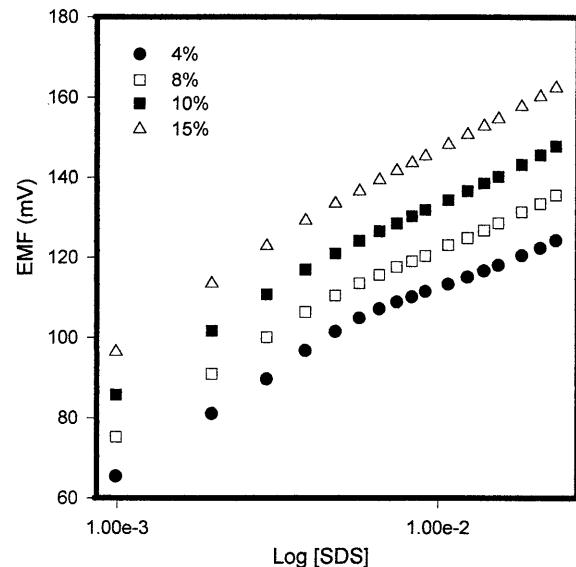


Fig. 3 Electromotive force (EMF) plots of the  $\text{Na}^+$ /double-junction reference electrode for SDS in 1,2-BTD/H<sub>2</sub>O mixtures

where the polarity of the microenvironment decreases sharply, resulting in a lower  $I_1/I_3$  value. We monitored the 1:3 ratio as a function of SDS concentration in various BTD/water mixtures. It must be noted that the characteristic vibrational fine structure of pyrene was not modified in the presence of diol and only slight changes in the intensity of the vibronic bands (1:3) were observed.

The cmc values were obtained from the abrupt change of curvature in the plots of  $I_1/I_3$  as a function of SDS (Fig. 4). The cmc values obtained from conductivity, fluorescence and potentiometric methods differ slightly from each other and an average value of the three is presented in Table 1 along with the values of  $\alpha$  obtained from conductometric and potentiometric methods.

In order to observe the dependency of the micellar properties on the characteristic solvent parameters, the cmc values of SDS in the binary mixtures were correlated with the partial molar volume ( $V_\phi$ ) and the compressibility ( $K_\phi$ ) values of BTDs in the binary mixture. These values were taken from our previous investigation [31]. Plots showing the dependence of the cmc of SDS on both  $V_\phi$  and  $K_\phi$  of BTD in the binary aqueous mixtures at a particular BTD composition are shown in Figs. 5 and 6. The linear behavior of these plots indicates that the micellar behavior of SDS is strongly dependent on the parameters of the isomeric diols that are sensitive to the hydrophobicity.

Micellar aggregation numbers and micellar sizes were determined by employing the steady-state fluorescence quenching method developed by Turro and Yekta [32]. The method is based upon the quenching of a

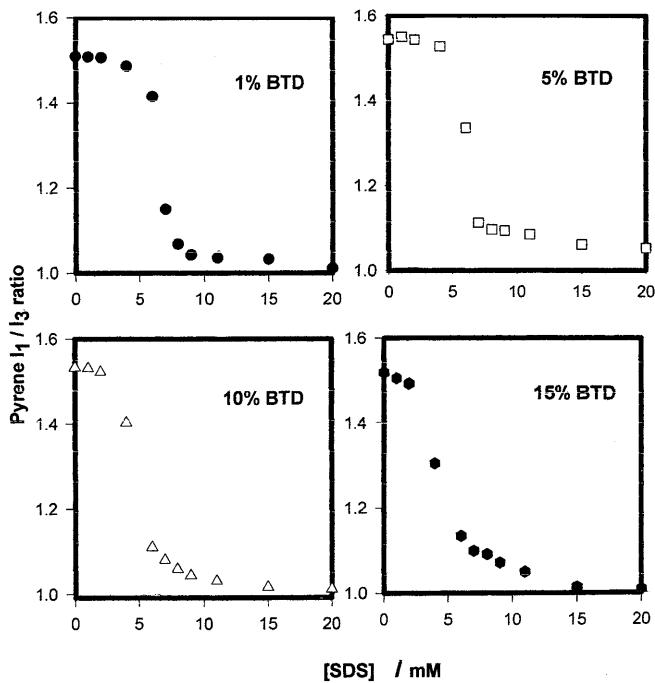


Fig. 4 Plots of pyrene 1:3 ratio versus concentration of SDS in aqueous solutions of 1,2-BTD

Table 1 Micellar properties of sodium dodecyl sulfate (SDS) in isomeric butanediol (BTD)/water mixtures. Method 1, conductometric; method 2, potentiometric. The estimated error in  $\alpha$  is  $\pm 0.05$

System	Wt%	cmc/cmc <sup>0</sup>	$\alpha$	
			Method 1	Method 2
1,2-BTD	0	1.00	0.39	0.38
	1.0	0.72	0.46	0.45
	3.5	0.62	0.52	0.52
	5.0	0.59	0.56	0.56
	7.5	0.56	0.62	0.62
	10	0.52	0.69	0.72
	15	0.50	0.78	0.81
1,3-BTD	1.0	0.78	0.40	0.39
	3.5	0.77	0.46	0.47
	5.0	0.76	0.48	0.48
	7.5	0.76	0.52	0.51
	10	0.75	0.58	0.54
	15	0.74	0.64	0.60
1,4-BTD	1.0	0.99	0.42	0.41
	3.5	0.90	0.47	0.45
	5.0	0.88	0.49	0.47
	7.5	0.84	0.54	0.50
	10	0.79	0.59	0.53
	15	0.78	0.67	0.56
2,3-BTD	1.0	0.72	0.34	0.33
	3.5	0.70	0.41	0.41
	5.0	0.67	0.45	0.44
	7.5	0.65	0.52	0.52
	10	0.62	0.57	0.58
	15	0.60	0.72	0.70

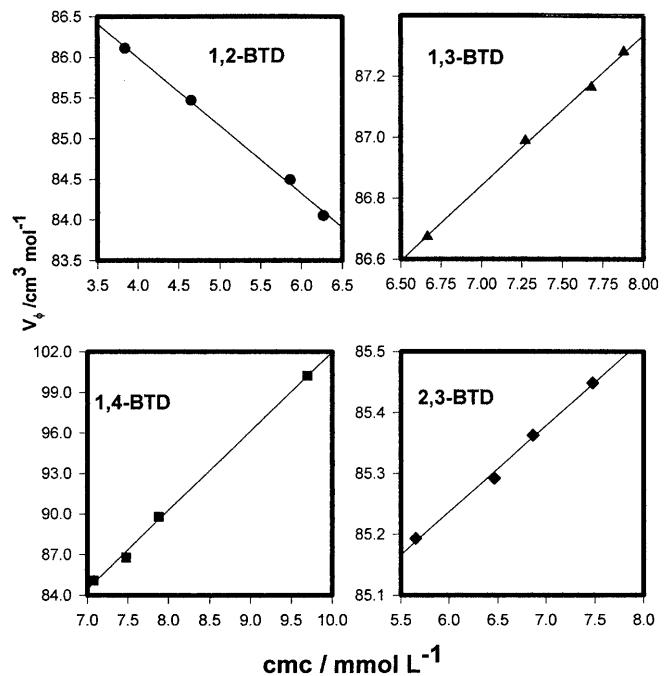


Fig. 5 Plots of critical micellar concentration (cmc) versus  $V_\phi$  of BTDs at 298 K

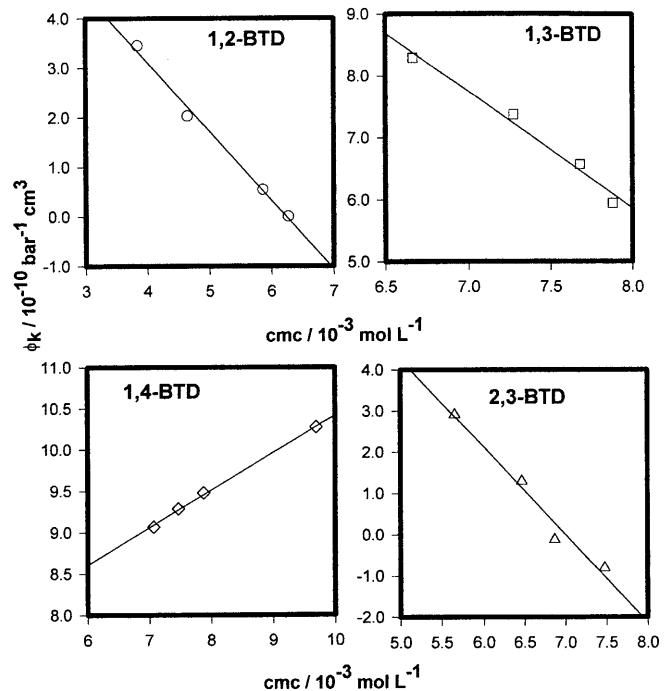


Fig. 6 Plots of cmc versus  $K_\phi$  of BTDs at 298 K

luminescence probe by a known amount of a quencher and has been applied successfully to the determination of mean aggregation numbers of SDS micelles in water and in the presence of additives [16, 24, 33].

In the present study the pyrene-hexadecylpyridinium ion pair was used to determine the aggregation number. This pair meets all the requirements for the determination of aggregation numbers by the static quenching method. The requirements are that the probe and the

quencher both be solubilized and immobile within the micelle, that the quenching rate be faster than the emission lifetime of the probe and that the distribution of the probe and the quencher among the micelles follow a Poisson distribution. The ratio of the luminescence intensities  $I_0/I$  without and with the quencher, Q, is related to the micelle concentration, [M], by the equation

$$\ln\left(\frac{I_0}{I}\right) = \frac{[Q]}{[M]} . \quad (2)$$

The micelle concentration is given by

$$[M] = \frac{S - cmc}{N_s} , \quad (3)$$

where  $S$  is the total surfactant concentration and  $N_s$  is the mean aggregation number. By combining Eqs. (2) and (3) we get

$$\ln\left(\frac{I_0}{I}\right) = \frac{N_s}{[S - cmc]} [Q] . \quad (4)$$

Plots of  $\ln\left(\frac{I_0}{I}\right)$  versus [Q] for all systems demonstrated good linearity (Fig. 7) and the mean aggregation numbers obtained from the value of the slopes are presented in Table 2. The experiments were repeated to check the reliability of the procedure. The  $I_1/I_3$  ratios of pyrene for the solvent system and in the presence of micelles are also presented in Table 2. From the examination of the  $I_1/I_3$  ratios in 0.05 M SDS in BTD (Table 2) it is apparent that the probe senses a relatively

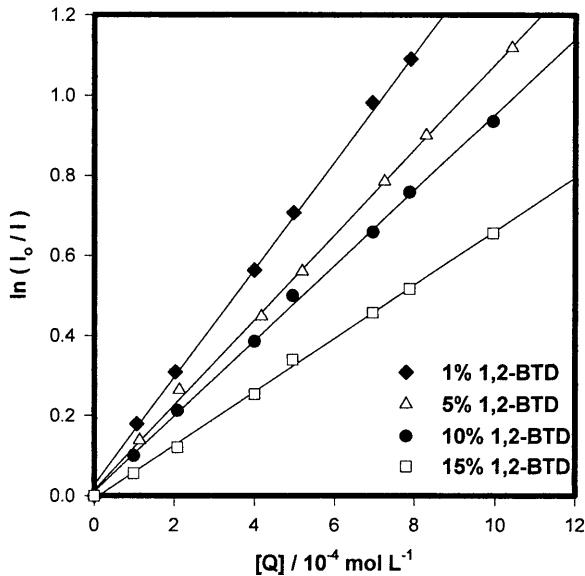
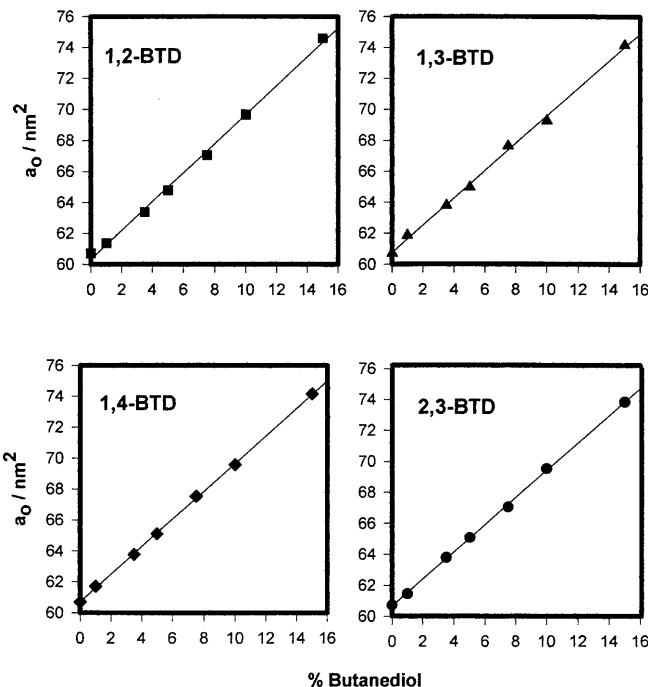


Fig. 7  $\ln(I_0/I)$  versus quencher concentration in binary mixtures of 1,2-BTD/water containing 50 mM SDS

**Table 2** Micellar parameters (the micellar radius calculated assuming spherical micelles,  $R$ , the surface area per headgroup,  $a_0$ , and the critical packing parameter,  $v/a_0 l_c$ ), aggregation numbers ( $N_s$ ) and  $I_1/I_3$  ratios

System	% BTD	$N_s$ ( $\pm 3$ )	$R$ (Å)	$a_0$ (Å $^2$ )	$v/a_0 l_c$	BTD	0.05 M SDS in BTD
1,2-BTD	0	62	17.3	60.7	0.35	1.82	1.24
	1.0	60	17.1	61.4	0.34	1.38	1.01
	3.5	52	16.3	64.4	0.33	1.35	1.02
	5.0	51	16.2	64.8	0.32	1.37	1.05
	10	46	15.7	67.1	0.31	1.37	1.03
	15	41	15.1	69.7	0.30	1.36	1.01
1,3-BTD	1.0	58	16.9	62.1	0.34	1.47	1.06
	3.5	56	16.7	62.8	0.33	1.45	1.05
	5.0	51	16.2	64.8	0.32	1.49	1.06
	7.5	49	16.0	65.7	0.32	1.51	1.05
	10	41	15.1	69.7	0.30	1.61	1.05
	15	34	14.2	74.2	0.28	1.58	1.07
1,4-BTD	1.0	59	17.0	61.7	0.34	1.47	1.06
	3.5	51	16.2	64.7	0.32	1.56	1.05
	5.0	48	15.9	66.1	0.32	1.58	1.06
	7.5	45	15.6	67.5	0.31	1.57	1.05
	10	43	15.3	68.6	0.32	1.58	1.07
	15	34	14.2	74.1	0.28	1.59	1.08
2,3-BTD	1.0	57	16.8	62.4	0.34	1.35	1.06
	3.5	51	16.2	64.7	0.32	1.36	1.04
	5.0	47	15.7	66.1	0.32	1.41	1.02
	7.5	44	15.4	66.6	0.30	1.34	1.02
	10	39	14.8	70.8	0.30	1.35	1.02
	15	35	14.3	73.4	0.29	1.41	1.01

lower polar environment in the micellar system of SDS containing diols. The various concentrations of the diols did not affect the polarity sensed by the probe.



**Fig. 8** Surface area per headgroup ( $a_0$ ) of SDS micelles versus diol composition

**Table 3** Thermodynamic properties of micellization. The units for  $\Delta G$  and  $\Delta H$  are kilojoules per mole with an error of  $\pm 0.5$  kJ and the units for  $\Delta S$  are joules per Kelvin per mole with an error of  $\pm 5$  J

BTD	Wt%	$\Delta'_M G_1^0$	$\Delta_{HP} G_1^0$	$\Delta_M G^0$	$\Delta_s G_1^0$	$\Delta_{HP} G_{11}^0$	$\Delta_s G_{11}^0$	$\Delta_M H^0$	$\Delta_M S^0$
1,2-BTD	0	-14.4	-23.5	-37.9	14.4	0.0	0.0	-1.8	121
	1.0	-11.6	-23.2	-34.8	11.6	0.3	-2.8	0.0	117
	3.5	-11.7	-21.5	-33.2	11.7	2.0	-2.7	1.2	107
	5.0	-11.7	-20.8	-32.5	11.7	2.7	-2.7	-4.9	93
	7.5	-11.6	-19.0	-30.6	11.6	4.5	-2.8	-4.8	86
	10	-11.6	-17.7	-29.3	11.6	5.9	-2.8	-8.2	71
	15	-11.7	-15.5	-27.2	11.7	8.0	-2.7		
1,3-BTD	1.0	-11.7	-23.6	-35.3	11.7	-0.1	-2.7	-0.1	118
	3.5	-10.1	-23.8	-33.9	10.1	-0.3	-4.3	-1.4	109
	5.0	-10.0	-22.3	-33.3	10.0	1.2	-4.4	-2.6	105
	7.5	-10.6	-21.6	-32.2	10.6	1.9	-3.8	-4.1	94
	10	-11.7	-19.4	-31.1	11.7	4.1	-2.7	-6.1	84
	15	-11.5	-17.6	-29.1	11.5	5.9	-2.9		
1,4-BTD	1.0	-11.7	-23.2	-34.9	11.7	0.3	-2.7	-0.4	116
	3.5	-11.4	-22.2	-33.6	11.4	1.3	-3.0	-2.0	106
	5.0	-11.3	-21.6	-32.9	11.3	1.9	-3.1	-4.9	94
	7.5	-11.2	-20.5	-31.7	11.2	3.0	-3.2	-9.2	76
	10	-11.2	-19.3	-30.5	11.2	4.2	-3.2	-8.3	75
	15	-11.7	-16.4	-28.1	11.7	7.1	-2.7		
2,3-BTD	1.0	-14.2	-22.2	-34.6	14.2	1.3	-0.2	0.2	117
	3.5	-13.8	-21.4	-35.2	13.8	2.1	-0.6	-1.2	114
	5.0	-12.0	-21.4	-33.4	12.0	2.1	-2.4	-2.9	102
	7.5	-11.6	-21.3	-32.9	11.6	2.2	-2.8	-5.8	91
	10	-10.0	-21.2	-31.2	8.9	1.2	-5.5	-7.8	79
	15	-7.4	-21.0	-28.4	6.0	1.1	-8.4		

The surface area per headgroup ( $a_0$ ) is known to be the controlling factor for micelle size [34]. The individual hydrophobic chain volume ( $v$ ) and the critical chain length ( $l_c$ ) can be obtained by employing Tanford's equation [35].

$$v = (27.4 + 26.9n)\text{Å}^3 \quad (5)$$

$$l_c = (1.5 + 1.265n)\text{Å} \quad (6)$$

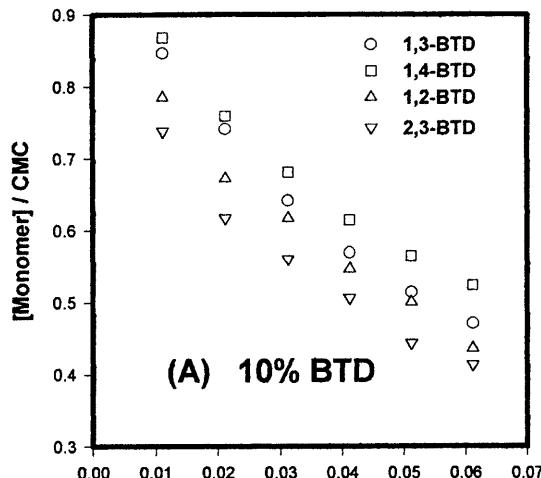
where  $n$  is the number of carbon atoms in the alkyl chain. By assuming spherical geometry, the micellar radius, surface area per headgroup and the critical packing parameter ( $v/a_0 l_c$ ) that controls the micelle shape were calculated and are presented in Table 2.

The area per headgroup increases linearly with the diol content (Fig. 8) and this may be attributed to the replacement of water molecules in the solvation layer of the micelle headgroup by diol molecules. The decrease in the critical packing parameter indicates that addition of diol favors the formation of smaller spherical micelles [36].

### Thermodynamics of micellization

The micellization of anionic surfactants may be described by





(A) 10% BTD

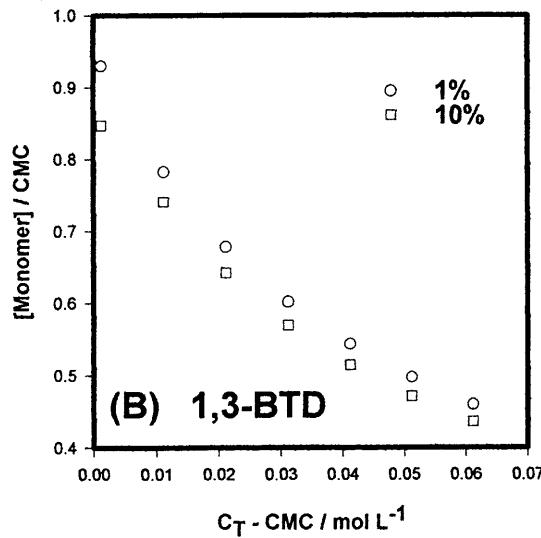


**Fig. 9 A** Plots of [monomer]/cmc versus  $c_T$ -cmc for 10% diols **B** Plot of [monomer]/cmc versus  $c_T$ -cmc at different percentages of 1,3-diol

where  $s^-$ ,  $c^+$  and  $M^{P^-}$  stand for monomer, counterion and micelle concentrations, respectively.

The equilibrium constant can be written in terms of the standard free-energy formation per monomer ( $\Delta_M G^0$ ) as follows:

$$\Delta_M G^0 = RT \left[ -\left(\frac{1}{n}\right) \ln a_{M^{P^-}} + \ln a_{s^-} + \left(1 - \frac{p}{n}\right) \ln a_{c^+} \right], \quad (8)$$

where  $a$  represents the activity of the species involved. In dilute solutions the activities can be replaced by concentrations (expressed in mole fraction units). The Gibbs energy of micellization,  $\Delta_M G^0$ , can be treated as the sum of the hydrophobic free energy of transfer of the surfactant monomer from the media to the interior,

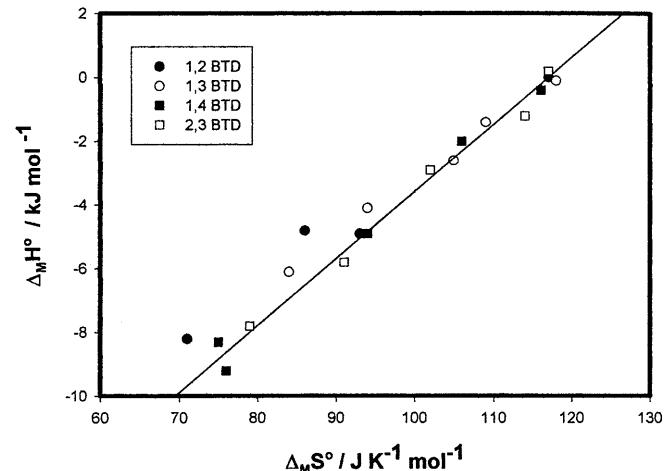


**Fig. 10** Plot of  $\Delta_M H^0$  versus  $\Delta_M S^0$  for various aqueous diol solution

$\Delta_{HP} G_{(1)}^0$ , and the energy associated with the surface contributions,  $\Delta_S G_{(1)}^0$ .

The value of  $\Delta_{HP} G_{(1)}^0$  is given by

$$\Delta_M G_{(1)}^0 = \Delta_{HP} G_{(1)}^0 = RT \left[ -\left(\frac{1}{n}\right) \ln X_{M^{P^-}} + \ln X_{S^-} \right]. \quad (9)$$

The energy associated with the surface contributions consists of electrostatic interactions between headgroups and the counterions along with other specific interactions and is given by

$$\Delta'_M G_{(1)}^0 = -\Delta_S G_{(1)}^0 = RT \left( 1 - \frac{p}{n} \right) \ln X_{c^+}. \quad (10)$$

By employing the mass-action model, the concentrations of monomers, counterions and micelles in the postmicellar region for SDS in the concentration range 0.02–0.10 M were calculated as outlined previously by us [24].

The values of  $\Delta_{HP} G_{(1)}^0$ ,  $\Delta_S G_{(1)}^0$  and  $\Delta_M G^0$  are presented in Table 3. The effect of the additive on the free energy of micellization can be calculated as follows:

$$\Delta_{HP} G_{(11)}^0 = \Delta_{HP} G_{\text{Diol}+\text{H}_2\text{O}}^0 - \Delta_{HP} G_{\text{H}_2\text{O}}^0 \quad (11)$$

$$\Delta_S G_{(11)}^0 = \Delta_S G_{\text{Diol}+\text{H}_2\text{O}}^0 - \Delta_S G_{\text{H}_2\text{O}}^0 \quad (12)$$

The values are also presented in the Table 3. The micellization enthalpies measured by solution calorimetry from our previous studies [25] were employed to calculate the entropies of micellization in these binary liquid mixtures and are listed in Table 3.

The overall difference in the hydrophobic free energy change ( $\Delta_{HP} G_{(11)}$ ) upon micelle formation increases with the diol content except for the 2,3-BTD system. This is attributed to the formation of mixed micelles and to the formation of small aggregates with highly solvated headgroups. The increase in the degree of dissociation is reflected in the negative values of  $\Delta_S G_{(11)}$ . The removal

of the counterions from the surface enhances the surface potential by increasing the electrostatic repulsion between the headgroups, which consequently destabilizes the micelles; however, in the present study this effect was minimized by the penetration of diols into the headgroup region of the micelles, which reduces the electrostatic repulsion.

The monomer concentrations in the postmicellar solution obtained by the mass-action model are plotted in Fig. 9A for 10% BTD content. The decrease in the monomer concentration follows the order 2,3 > 1,2 > 1,3 > 1,4 BTDs. For a given diol, the monomer concentration decreases with increasing diol content (Fig. 9B).

The enthalpies of micellization versus the entropies of micellization for all diols gave a fairly linear plot with a compensation temperature of 210 K (Fig. 10), which is an interesting phenomenon. The addition of cosolvent lowers the entropy and enthalpy changes (Table 3), which shifts of the curves to regions of smaller entropy change and more negative enthalpy change. In the present study similar behavior was observed for all isomeric diols of varying composition and hence a single slope was obtained. On the basis of these observations, it can be concluded that the micellization of SDS in these

binary mixtures is still a compensation process and is different from pure water and other aqueous systems [37, 38].

## Conclusions

The decrease in the cmc and the aggregation numbers with the addition of diols can be attributed to the increase in the solvophobic effect and to the formation of mixed micelles. This effect varies in the order 1,2 > 2,3 > 1,3 > 1,4 BTDs. It is apparent that the position of the second hydroxyl group has an effect on the micellar properties. The increase in the effective degree of dissociation with diol content is due to the decrease in charge density at the micellar surface caused by the increase in the surface area per headgroup and the decrease in aggregation number. Intermicellar properties obtained from the mass-action model may prove to be useful in the interpretation of kinetic data on monomer/micelle equilibria and solubilization process.

**Acknowledgements** This research was supported by a grant to R.P. from the Natural Sciences and Engineering Research Council of Canada (NSERC). S.E.B. acknowledges the Undergraduate Summer Research Award from the NSERC (1998).

## References

1. Hovanec JW, Wong NM, Longo FR (1995) 16:543–555, and references therein
2. Holmberg K, Laughlin RG (1997) *Curr Opin Colloid Interface Sci* 2:453–455
3. Wärnheim T (1997) *Curr Opin Colloid Interface Sci* 2:472–477
4. Beesby A, Evans DF, Laughlin RG (1988) *J Phys Chem* 92:791–793
5. Friberg SE, Ward JI, Larsen DW (1987) *Langmuir* 3:735–737
6. Palepu R, Gharibi H, Bloor DM, Wyn-Jones E (1993) *Langmuir* 9:110–112
7. Jonströmer M, Sjöberg M, Wärnheim T (1990) *J Phys Chem* 94:7549–7555
8. Ylihautala M, Vaara J, Ingman P, Johisaari J, Diehl P (1997) *J Phys Chem B* 101:32–38, and references therein
9. Perche T, AuVray X, Petipas C, Anthore R, Rico-Lattes I, Lattes A (1997) *Langmuir* 13:1475–1480
10. Ray A (1971) *Nature* 231:313–315
11. Backlund S, Bergenstahl B, Molander O, Wärnheim T (1989) *J Colloid Interface Sci* 131:393–401
12. Binana-Limbele W, Zana R (1989) *Colloid Polym Sci* 267:440–447
13. Sjöberg M, Henriksson V, Wärnheim T (1990) *Langmuir* 6:1205–1211
14. Gharibi H, Palepu R, Bloor DM, Hall D, Wyn-Jones E (1992) *Langmuir* 8:782–787
15. Callaghan A, Doyle R, Alexander E, Palepu R (1996) *Langmuir* 9:3422–3426
16. Gracie K, Turner DW, Palepu R (1996) *Can J Chem* 74:1616–1625
17. Zana R, Yiv S, Strazielle C, Lianos P (1981) *J Colloid Interface Sci* 80:208–222
18. Armstrong DW, Henry SJ (1980) *J Liq Chromatogr* 3:657–662
19. Terabe S, Otsuka K, Ichikawa K, Tsuchiya A, Ando T (1984) *Anal Chem* 56:111–113
20. Saz JM, Marina ML (1994) *J Chromatogr* 687:1–12
21. Blokhus AM, Høiland H, Backlund S (1986) *J Colloid Interface Sci* 114:9–15
22. Høiland H, Blokhus AM (1990) In: Bloor DM, Wyn-Jones E (eds) *The structure, dynamics and equilibrium properties of colloidal systems*. Kluwer, Boston, pp 39–48
23. Canadas O, Valiente M, Rodenas E (1998) *J. Colloid Interface Sci* 203:294–298
24. Turner D, Gracie K, Taylor T, Palepu R (1998) *J. Colloid Interface Sci* 202:359–368
25. McMahon CA, Hawrylak B, Marangoni DG, Palepu R (1999) *Langmuir* 15:429–436
26. Moroi Y (1988) *J Colloid Interface Sci* 122:308–314
27. Gracie K, Wiseman P, Palepu R (1999) *Phys Chem Liq* 37:107–123
28. Kalyanasundaram K (1987) *Photochemistry in microheterogeneous systems*. Academic, New York, pp 36–96
29. Griseri F, Drummond CJ (1988) *J Phys Chem* 92:5580–5593
30. Kalyanasundaram K, Thomas JK (1977) *J Am Chem Soc* 99:2039–2044
31. Hawrylak B, Gracie K, Palepu R (1998) *J Solution Chem* 27:17–31
32. Turro NT, Yekta A (1978) *J Am Chem Soc* 100:5951–5952
33. Lissi EA, Aubin E (1985) *J Colloid Interface Sci* 105:1–6
34. Israelachvili JN (1985) In: Degiorgio V, Corti M (eds) *Physics of amphiphiles: micelles, vesicles and microemulsions*. North Holland, Amsterdam, pp 42–59
35. Tanford C (1980) *The hydrophobic effect*. Wiley, New York, pp 42–59
36. Brigandt P, Puvvada S, Blankschtein D (1991) *J Phys Chem* 95:8989–8995
37. Lee DJ, Huang WH (1996) *Colloid Polym Sci* 274:160–165
38. Sugihara G, Hisatomi M (1999) *J Colloid Interface Sci* 219:31–36